Experimental and numerical analysis of underwater consolidation of dredged sediment
a case of study for the Marker Wadden

Barciela-Rial, Maria; van den Bosch, Barend A. P.; van Kessel, Thijs ; Griffioen, Jasper; Winterwerp, Johan C.

Important note
To cite this publication, please use the final published version (if applicable).
Please check the document version above.

Experimental and numerical analysis of underwater consolidation of dredged sediment: a case of study for the Marker Wadden

Maria Barciela-Rial[1,2], Barend A. P. van den Bosch[3],
Thijs van Kessel[4], Jasper Griffioen[5,6] and Johan C. Winterwerp[1*]

[1]Built Environment Academy, HAN University of Applied Sciences, Arnhem, Netherlands, [2]Hydraulic
Engineering, Faculty of Civil Engineering and Geosciences, Delft University of Technology,
Delft, Netherlands, [3]Environmental Engineering, Van Oord, Rotterdam, Netherlands, [4]Marine and
Coastal Systems, Deltares, Delft, Netherlands, [5]Copernicus Institute of Sustainable Development,
Faculty of Geosciences, Utrecht University, Utrecht, Netherlands, [6]Hydrology and Reservoir
Engineering, TNO Geological Survey of the Netherlands, Utrecht, Netherlands

Dredged sediments, which are mud suspensions with concentrations exceeding
the gelling point, are utilised in reclamation and Building with Nature projects.
Beyond the gelling point, flocs occupy space and begin to form a network
structure. This study investigates the impact of initial conditions, specifically the
concentration above the gelling point and the stress state, on the consolidation
of dredged sediment. The sediment from Lake Markermeer in the Netherlands
was studied, specifically in the context of the construction of the Marker Wadden
wetland. Material parameters were determined using two distinct experimental
methods: settling columns and Seepage Induced Consolidation (SIC) tests. The
differences observed between the two sets of material parameters suggest that
the stress history and plastic deformation during mixing may influence the
results. These effects were analysed using a one-dimensional vertical (1DV)
consolidation model. The computed profiles were then compared with the
profiles measured using an Ultrasonic High Concentration Meter. An initial
concentration of 558.1 g/l, achieved by remixing the equilibrium profile of a
normally consolidated suspension, resulted in larger final densities and a lower
sediment-water interface. Conversely, a concentration of 175.6 g/l, achieved by
remixing consolidating dredged sediment, yielded the same equilibrium layer
thickness and density profile as virgin consolidation, albeit after a longer
consolidation time. These findings are particularly relevant for land reclamation
and wetland construction projects, where the initial density may be high and the
dredging process's mixing may alter the stress state.

1 Introduction

A cohesive sediment-water mixture can behave as a dense fluid, when the pore pressure is equal to the total stress, or as a soft soil, when the pore pressure is lower than the total stress and therefore effective stress builds up (Terzaghi, 1923; Terzaghi and Peck, 1967). The density at which effective stress develops is referred as structural density (Sills, 1998) or gelling point (Winterwerp, 1999; Dankers, 2006). At the structural density, flocs are space-filling and a network structure starts to build-up. The mass concentration of solids at this point is referred as gelling concentration (c_{gel}).

Dredged sediment at concentrations above the gelling point are used for reclamation and Building with Nature (BwN) projects. The Marker Wadden project in The Netherlands is an example of a BwN project using dredged sediment, originating from the sediment deposited in Lake Markermeer, to create a new wetland in the lake (Barciela-Rial et al., 2020, 2022, 2023). In order to use the sediment of the lake bed, it has to be diluted with water so that it can be pumped. The dredged sediment is placed in calm areas where they are allowed to settle and consolidate. In this paper the effect of the initial concentration on the final density profile and bed height was studied.

The settling and consolidation behaviour of mud at initial concentrations below this gelling point has been thoroughly studied by various authors (e.g. Gibson et al., 1967; Been and Sills, 1981; Toorman, 1999; Merckelbach, 2000; Dankers, 2006; De Lucas Pardo, 2015). It was shown that the material parameters can be determined from simple settling column experiments (Merckelbach and Kranenburg, 2004a). Such material parameters can be used to calculate the hydraulic conductivity and effective stress from equations based on the volumetric concentration of solids (Merckelbach and Kranenburg, 2004b). However, the consolidation behaviour of mixtures above the gelling point, as it is the case for dredged sediment, has been less studied and determination of the material characteristics requires more sophisticated experimental devices. Imai (1979) proposed a Seepage Induced Consolidation (SIC) test in which a downward seepage is imposed by creating a constant head difference. Herein, pore water pressures are continuously measured and the void ratio

is obtained at the end by slicing the sample. This method was later improved by Znidarčić and Liu (1989). In this improved configuration, a constant flow rate is imposed across the sample instead of a constant head. This enables testing under small gradients leading to more reliable results at the low effective stress ranges of soft cohesive soils. The SIC test allows to obtain void ratio-hydraulic conductivity and void ratio-effective stress relations (Huerta et al., 1988; Liu and Znidarčić, 1991).

The initial concentration of solids c_0 at which a settling test is performed may influence the settling and consolidation behaviour of the sediment. An hypothetical settling experiment started by remixing the final density (equilibrium) profile over the final bed height h_∞ of a virgin consolidated suspension ($c_0 < c_{gel}$) has c_0 significantly larger than c_{gel}. In a similar way, when remixing at an earlier phase of consolidation, c_0 may still be above c_{gel}. In both mixing situations shown in Figure 1, there is a mismatch between the *in-situ* stresses and the at-rest virgin consolidation behaviour. We refer as "slurry" to a mixture of dredged sediment with an initial concentration above gelling point, as it is the case for dredged sediment. The top part of such mixed slurry is over-consolidated. This implies that there is not an equilibrium between the vertical stresses, the local strength and the pore water pressure. The upper over-consolidated part has a lower water content w% and hydraulic conductivity than the original suspension equilibrium profile. This upper part has a larger density and is less permeable, thus acts as a "crust" over the -consolidating part. Water in the lower part can therefore not escape in the vertical direction as easy as in the case of a low concentrated suspension.

In classical soil mechanics unloading tests, negative pore pressures would result in elastic rebound of the material, often referred to as swelling (e.g. Lambe and Whitman, 1969). During the Constant Rate of Strain tests performed by Barciela-Rial (2019) and Barciela-Rial et al. (2022), this elastic rebound was not induced because negative pore pressures were prevented. Therefore, only the microscopic swelling of clay particles was measured. The coefficients of swelling determined in Barciela-Rial (2019) are thus applicable to the consolidation dredged sediment studied in the present paper.
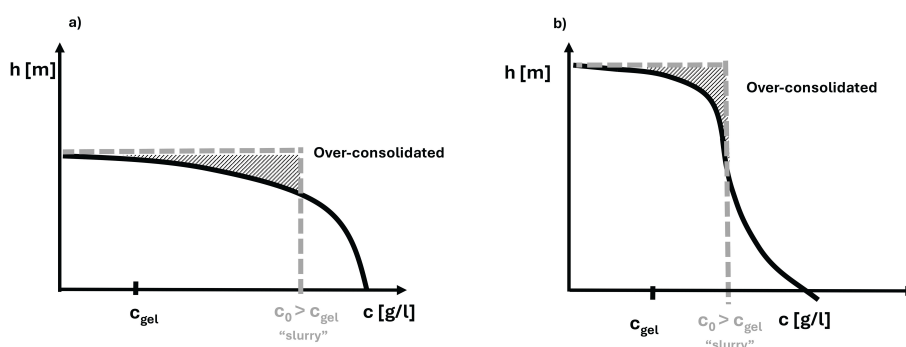
FIGURE 1
(A) Initial concentration(c_0) profile for a slurry after remixing the final equilibrium concentration profile obtained from a suspension by virgin consolidation. **(B)** Initial concentration profile for a slurry after remixing the concentration profile during the first stages of consolidation. The initial sediment concentration c_0 is now smaller than in the previous case. However, $c_0 > c_{gel}$ for both cases. X-axis represents the concentration. Y- axis represents the height.

In the present paper, the effect of the initial concentration c_0 on the consolidation behaviour of mud was studied for mud mixtures with an initial concentration above the gelling point. This effect was analysed with a 1DV consolidation model. For that, the material parameters were calculated for $c_0 > c_{gel}$ with the Seepage Induced Consolidation test (Liu and Znidarčić, 1991) and compared with the results obtained from settling columns for $c_0 < c_{gel}$.

2 Methods

2.1 Sediment used

The type of Markermeeer sediment used in this paper is referred to as NE1F, which detailed composition is presented in Barciela-Rial (2019). Sample NE1F represents the fine fraction of a natural sample of the upper layer of sediment from the Northeast of Lake Markermeer. NE1F has 0% sand, 4.5% Total Organic Matter and a particle density ρ_s of 2540kg/m^3.

Various authors have determined the gelling concentration for different Markermeer sediment samples. The lowest value was obtained by De Lucas Pardo (2015), who found a c_{gel} of 70 g/l, while Hendriks (2016) obtained the highest value, with 85 g/l.

2.2 Experimental methods

The material parameters of Markermeer mud were obtained with two different experimental methods: settling columns (for $c_0 < c_{gel}$) and Seepage Induced Consolidation (SIC) tests (for $c_0 > c_{gel}$).

The settling column tests were performed at concentrations below c_{gel} (40, 50 and 60 g/l) and above (100, 200, 300 and 400 g/l), and replicate columns were included to assess reproducibility (See Figure 2). At the end of the settling column tests, the density profiles of all columns were measured with an Ultrasonic High Concentration Meter (UHCM). The UHCM measures high concentrations of solid particles in liquids. Figure 2 shows the set-up of the UHCM measuring in the column. The measurement is

based on the transmitting and receiving sound between two acoustic transducer. The acoustic principle is based on measuring the transmission of acoustic energy (ultra sound) through the measuring volume between the transmitter and the receiver probes. Details on the calibration and measurement procedure can be found in the Supplementary Materials.

For the columns with 200, 300 and 400 g/l, the material parameters were determined with the SIC test after the settling column tests were finished. This was done by placing the remoulded final settled bed of each column in the SIC ring for testing.

2.2.1 Material parameters for initial concentrations below gelling point

The material parameters for initial concentrations c_0 below the expected gelling point (De Lucas Pardo, 2015; Hendriks, 2016) were determined with settling column experiments. This is done in 2 litre columns with a height of 45 cm and an inner diameter of 8 cm (Figure 2). To initiate the experiment, each column is gently stirred vertically using a mixing rod. Each column is mixed with an identical number of strokes for the same duration, following a standardised protocol. This ensures an uniform treatment and reproducible results. This reproducibility was checked by performing two duplicate settling column tests for 200 and 400 g/l. Photographs of the columns are taken continuously to identify the sediment-water interface.

From the settling column experiments, the effective velocity w_s of the settling interface can be obtained from the slope of the settling curve. Dankers and Winterwerp (2007) established a relationship between w_s and the volumetric concentration of flocs ϕ_f:

$$w_s = w_{s,0} \frac{(1 - \phi_f)^m (1 - \phi_s)}{1 + 2.5\phi_f} \qquad (1)$$

where $w_{s,0}$ is the settling velocity of one individual particle in still water and $\phi_s = c/\rho_s$ is the volumetric concentration of solids (primary particles), in which c is the mass concentration and ρ_s the particle density. The volumetric concentration of flocs ϕ_f is equal to c/c_{gel} because $\phi_f = \phi_s/\phi_{gel}$ by definition. The empirical parameter m
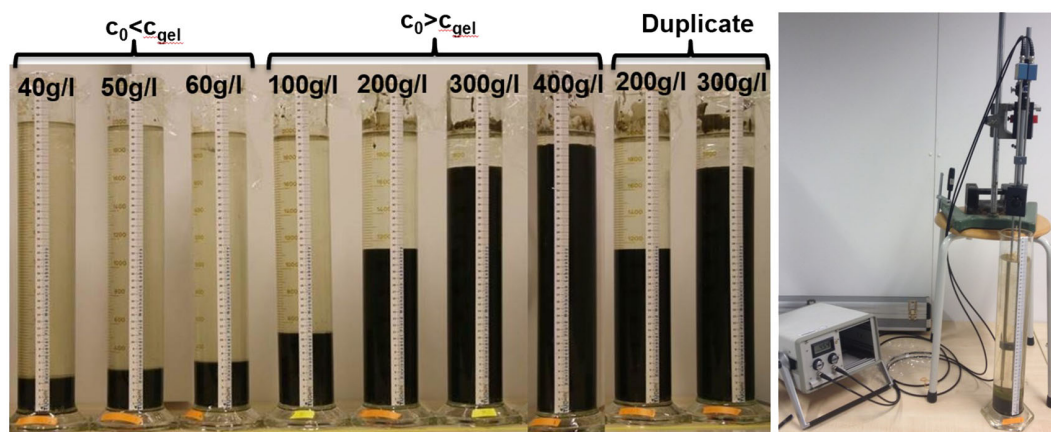

FIGURE 2
Settling column experiments performed and concentrations (left) and UHCM final density profile measurement (right).

that accounts for non-linearity was set to 2, according to Dankers and Winterwerp (2007). From two settling curves started at two different concentrations, the unknown variables $w_{s,0}$ and c_{gel} were calculated.

Assuming that the cohesive sediment flocs and bed behave as self-similar fractal structures (Kranenburg, 1994), the material parameters were obtained from the settling column experiments. The calculation was done according to Merckelbach and Kranenburg (2004a). First, the sediment- water interface during the first phase of consolidation, when the effective stresses are still small, was plotted and the following equation was fitted:

$$ h(t) - \zeta_s^{sa} = \left(\frac{2-n}{1-n} \zeta_s^f \right)^{\frac{1-n}{2-n}} (n-2) K_k \left(\frac{\rho_s - \rho_w}{\rho_w} \right)^{\frac{1}{2-n}} t^{\frac{1}{2-n}} \quad (2) $$

where ρ_w is the density of water, ζ_s^{sa} is the Gibson height accounting for sand (particles > 63μm) and ζ_s^f is the Gibson height of the fines fraction (particles < 63μm). ζ_s^f is equal to $\phi_s^f H_0$, where ϕ_s^f is the initial volumetric concentration of fines and H_0 the initial thickness of the slurry layer. Because the sediment studied did not contain sand, the volumetric concentration of sand $\phi_s^{sa}=0$ and $\zeta_s^{sa}=0$. Further, $h(t)$ [m] is the height of the mud-water interface, t [s] is the time and K_k [m/s] is the permeability material parameter, see Equation 4. The scalar n is related to the fractal dimension n_f as $n = 2/(3 - n_f)$. Next, the effective stress parameter K_σ was calculated, from equilibrium conditions, with Equation 3:

$$ h_\infty - \zeta_s^{sa} = \frac{n}{n-1} \frac{K_\sigma}{g(\rho_s - \rho_w)} \left(\frac{g(\rho_s - \rho_w)}{K_\sigma} \zeta_s^f \right)^{\frac{n-1}{n}} \quad (3) $$

where h_∞ is the final consolidation height and K_σ [Pa] is the effective stress material parameter.

The permeability and effective stress material parameters, K_k and K_σ, are used to calculate the hydraulic conductivity k and effective stress sigma $_{eff}$ of the sediment according to Equation 4 and Equation 5 (Merckelbach and Kranenburg, 2004b):

$$ k = K_k \left(\frac{\phi_s^f}{1 - \phi_s^{sa}} \right)^{-\frac{2}{3-nf}} \quad (4) $$

$$ \sigma_{\text{eff}} = K_\sigma \left(\frac{\phi_s^f}{1 - \phi_s^{sa}} \right)^{\frac{2}{3-nf}} \quad (5) $$

2.2.2 Material parameters for initial concentrations above gelling point

The material parameters for initial concentrations c_0 above the gelling point were determined with the SIC test device available at Deltares, Delft. The device used is based on Znidarčić and Liu (1989) and Abu-Hejleh et al. (1996). The set-up consists of a frame, a triaxial cell, a volume displacement pump, water supply cells, pressure, force and displacement transducers and a data acquisition system. For details on the SIC device we refer to the previous references, Znidarcic (1982) and the Supplementary Materials.

The samples tested in the SIC tests originated from the settling column experiments. After equilibrium was attained in each settling

column, the supernatant water was removed and the remaining sediment was transferred to a container in which it was gently mixed to homogenize, avoiding air entrapment. The water content was then determined by drying a subsample in an oven at 105°C to derive the initial void ratio e_0. Then, the sediment was put into the sample holder ring of the triaxial cell and allowed to rest for three days. The triaxial cell was filled with water to extrude air and the test was started. Three SIC tests were performed. They are referred as SIC200, SIC300 and SIC400 because the sediment originated from the settling columns with initial concentration 200, 300 and 400 g/l, respectively. There was not enough sediment in the column with $c_0 = 100$ g/l to fill in the SIC sampling ring.

To obtain compressibility and hydraulic conductivity data, each SIC test was run for seven loading steps followed by permeability steps. These loading and permeability steps are listed in Table 1. The loading steps were undrained at the bottom of the sample to allow measurement of the excess pore water pressure in time. After equilibrium was reached and the pressure stabilised (i.e., excess pore water was close to zero), a permeability step was applied by imposing a small downward water flux through the sample. The downward flow of water consolidates the sample, increasing the pressure difference across the sample with time. The same flow rate was maintained until steady state conditions were reached, no further consolidation occurred and the pressure difference across the sample became constant.

The void ratio was calculated continuously from the sample height during the tests and the initial void ratio e_0. At the end of the test, the final void ratio e_∞ was determined by oven-drying of a subsample at 105°C. The data was fitted to power law functions to obtain the hydraulic conductivity and effective stress. Here, two sets of power law functions were used. The first set was dependent on the volumetric concentration ϕ_s and consisted of the equation with the fractal descriptions used for the settling columns, i.e., Equation 4 and Equation 5. The second set was a function of the void ratio e and consisted of the following equations (Liu and Znidarčić, 1991):

$$ k = C_k e^{D_k} \quad (6) $$

$$ \sigma_{\text{eff}} = \left(\frac{e}{A_\sigma} \right)^{-\frac{1}{B_\sigma}} \quad (7) $$

where A_σ, B_σ, C_k and D_k are empirical parameters obtained from fitting. The void ratio e and the volumetric concentration of sediment ϕ_s (in this case $\phi_s = \phi_s^f$) are related as $1+e = 1/\phi_s$. For convenience, Equation 7 is also presented as:

$$ e = A_\sigma \sigma_{\text{eff}}^{-B_\sigma} \quad (8) $$

2.3 The 1DV-slurry model

To compare the behaviour of suspensions ($c_0 < c_{\text{gel}}$) with the one of dredged sediments or slurries ($c_0 > c_{\text{gel}}$), the two sets of parameters obtained from the settling columns and from the SIC tests were used as input for a the 1DV-slurry model to compute density profiles. This 1DV-slurry model is a version of the 1DV

TABLE 1   Seepage Induced Consolidation test plan including all the loading and permeability steps performed to each sample.

Step	Load	Stress	Discharge
	[N]	[Pa]	[mm^3/s]
Loading (filter stone)	1.8	98.5	
Loading	2.0	111.7	
Permeability (seepage)			0.5
Permeability (seepage)			1.0
Loading	5.0	279.2	
Permeability (seepage)			2.0
Permeability (seepage)			1.0
Loading	10.0*	558.4	
Permeability (seepage)			1.0
Permeability (seepage)			1.5
Loading	50.0	2792.1	
Permeability (seepage)			1.0
Permeability (seepage)			1.5
Loading	100.0	5584.0	
Permeability (seepage)			1.0
Permeability (seepage)			1.5
Loading	500.0	27920.7	
Permeability (seepage)			1.5
Permeability (seepage)			1.0
Permeability (seepage)			0.2
Permeability (seepage)			0.3
Loading	900.0	50257.3	
Permeability (seepage)			0.3
Permeability (seepage)			0.2
Permeability (seepage)			0.2
Permeability (seepage)			0.1

*For the SIC400, a load of 30 kPa was applied instead of 10 kPa.

model (Winterwerp, 1999; Winterwerp and van Kesteren, 2004) adapted for highly concentrated mixtures (i.e., dredged sediment).

2.3.1 Theoretical background

Winterwerp and van Kesteren (2004) rewrote the Gibson equation into an advection-diffusion equation, which is resolved on a rigid, vertically staggered grid. This implies that the height of settling/consolidating suspension is fixed to its initial height. Thus, the interface of the water-sediment suspension moves through the computational grid. This then requires an upwind numerical scheme and high resolution of the numerical model accounting for the sharp gradients at the interface. The advantage of this rigid grid approach is that sedimentation on and erosion from that

interface can be modelled easily, which is not the case when using Gibson's material coordinates.

This advection-diffusion consolidation equation reads, after introduction of the fractal approach (Equations 4, 5) and for the case when only fine particles ($\phi_s^f = \phi_s$), as follows

$$\frac{\partial \phi_s}{\partial t} - \frac{\partial}{\partial z}\left(\frac{\rho_s - \rho_w}{\rho_w} k\phi_s^2\right) - \Gamma_c \frac{\partial^2 \phi_s}{\partial z^2} = 0 \qquad (9)$$

where Γ_c is a consolidation coefficient defined as

$$\Gamma_c = \frac{2}{3 - n_f} \frac{K_k K_\sigma}{g\rho_w} \qquad (10)$$

In the present work, this model was further adapted to account for the compaction of highly concentrated mixtures such as dredged sediment. We refer to the resulting model as the 1DV-slurry. For the case of highly concentrated mixtures such as dredged sediment, the over-consolidated layer in the upper part of the mixture acts as a crust, reducing the outflow of excess pore water from the lower, consolidating part of the slurry. This reduction is modelled in the 1DV-model by reducing the consolidation coefficient Γ_c by a factor 100 in the crust. Thus for $c_0 < c_{gel}$: $\Gamma_{c,\,crust} = 0.01\Gamma_c$. In theory, this reduction can also be realised by reducing the hydraulic conductivity within the crust, maintaining the magnitude of the consolidation coefficient. However, numerical experiments showed that the model then becomes too diffusive, smearing out the sediment concentration over the layer thickness (Winterwerp et al., 2021). The effect of the crust is therefore modelled by adjusting the consolidation coefficient in the crust only. We refer to the swelling coefficient for convenience, appreciating that the 1DV-model cannot predict swelling.

The unloading or swelling behaviour of Markermeer sediment was experimentally quantified in Barciela-Rial (2019), where the swelling coefficient c_{sw} was obtained from unloading cycles during Constant Rate of Strain tests. For the material studied in the present paper, a value of $c_{sw} = 0.015$ was found. This small value implies that only little (elastic) rebound occurs upon loading.

2.3.2 Modelling approach

The numerical experiment included remixing of suspensions ($c_0 < c_{gel}$) up to the bed-water interface. As a result, the new settling material had a new initial concentration profile ($c_0 > c_{gel}$). The maximum time step in the computations was limited by the settling velocity and the size of the computational layers.

The density profiles computed with the 1DV-slurry model were then compared with the profiles measured with the Ultrasonic High Concentration Meter (UHCM) at the end of all the settling experiments. This allowed to validate the model.

The sensitivity of the model results was evaluated by also using the material properties obtained from the different experimental set-ups (SIC and settling columns).

Prognostic simulations were performed to test the influence of over-consolidation induced by the initial density profile. They consisted of remixing the density profile at equilibrium and at the second phase of consolidation.

3 Results

3.1 Material parameters for initial concentrations below gelling point

Figure 3 shows the settling curves for the tests below the gelling point. The slopes during the hindered settling phase (i.e. first minutes of the test) correspond with an effective velocity w_s of $3.95 \cdot 10^{-6}$, $2.19 \cdot 10^{-6}$ and $1.50 \cdot 10^{-6}$ m/s for $c_0 = 40$, 50 and 60 g/l respectively.

The pairs $w_{s,0}$ - c_{gel} obtained with Equation 1 are shown in Table 2. From these results, the intermediate gelling concentration value of 92.2 g/l was used for the subsequent calculations. The material parameters obtained with the fractal approach are shown in Table 3.

The density profiles measured at the end of the settling column tests with $c_0 < c_{gel}$ are shown in Figure 4. The overshoots observed on these data are due to inaccuracies of the UHCM device near the interface.

3.2 Material parameters for initial concentrations above gelling point

Figure 5 shows the consolidation curves for the tests with initial concentrations above the gelling point and the density profiles which were measured with the UHCM device at the end of the tests. The consolidation curves for $c_0 > c_{gel}$ showed an initial linear phase caused by a higher density than at equilibrium in the upper part of the mud layer (over-consolidated). This excess density caused the upper layer to be heavier and less permeable and therefore act like a crust.

For the columns with 200, 300 and 400 g/l, the material parameters were determined with the SIC tests after the settling column tests were finished. The results from the SIC tests as a function of ϕ_s are shown in Figure 6. From fitting the fractal Equations 4, 5, the material parameters presented in Table 4 were obtained. The fact that these material parameters obtained from the SIC test are not identical to the ones determined from the settling column tests suggests an influence of the stress history and plastic deformation upon remixing of the settled bed when preparing the

TABLE 2 Gelling concentrations and sediment particle velocity of the sediment studied for $c_0 < c_{gel}$ settling experiments.

c_{gel} [g/l]	$w_{s,0}$ [m/s]
95.1	2.30E-03
92.2	2.61E-03
88.5	2.84E-03

sample for the SIC test. This may induce over-consolidated behaviour during the SIC tests. The different initial concentrations at which settling columns and SIC tests were performed, may also have influenced these results.

The material parameters calculated according to Liu and Znidarčić (1991) are also shown in Table 4. They were obtained from fitting Equations 6, 8 to the results as a function of the void ratio (see Figure 7). Note that the comparison of the set of Equations 4, 5 with Equations 6, 7 yields to the following approximate equation to calculate D_k:

$$D_k = \frac{n_f}{B_\sigma} \tag{11}$$

which gives values of D_k of the same order of magnitude that presented in Table 4.

3.3 The 1DV-slurry model

3.3.1 Validation of the model

The density profiles computed with the 1DV-slurry model were compared with the profiles measured with the Ultrasonic High Concentration Meter (UHCM) at the end of the settling experiments after 67 days. This was done for initial concentrations of 200 and 300 g/l. Figure 8 shows that there is a good agreement between the measured and computed density profiles where the latter were calculated using the SIC parameters. However, there is some difference near the bottom of the column, where the UMHC measurement profile becomes concave-up. Furthermore, the agreement between the profile computed with the settling column parameters from $c_0 = 40$ g/l showed offset with
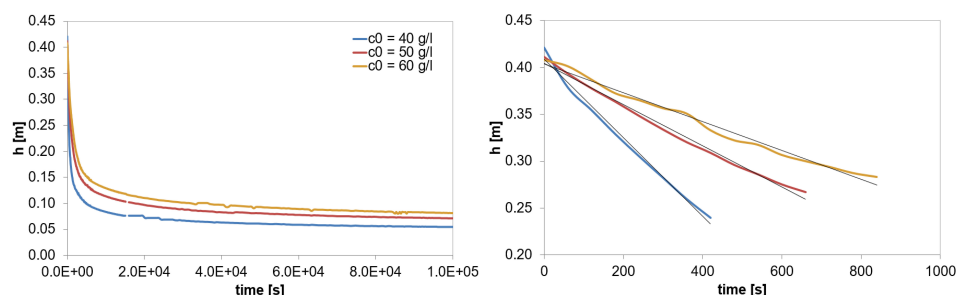

FIGURE 3
Settling curves for the experiments at $c_0 < c_{gel}$ (left) and zoom in during the hindered settling phase (right). The black line in the right figure is a linear trend line of all the data points, which is used to calculate the effective settling velocity.

c_0 [g/l]	n_f [-]	K_k [m/s]	$h\infty$ [m]	K_σ [Pa]
40	2.70	1.23E-13	4.3E-02	1.12E+07
50	2.69	2.18E-13	5.3E-02	8.10E+06
60	2.70	1.74E-13	6.2E-02	1.26E+07

respect to the measured profile for the case of c_0 = 300 g/l. In particular, the computed profile with these parameters did not indicate equilibrium at t = 67 days. This suggests that the offset may be caused by the permeability coefficient K_k from the settling columns, which was one order of magnitude smaller than the corresponding SIC parameter. Thus, even if final bed heights may be predicted correctly when using the different sets of material parameters, the consolidation time may vary considerably due to differences of the K_k values (Barciela-Rial, 2019).

The results show that the determination of the material parameters with the SIC tests provide more accurate results of the settling and consolidation of mixtures with $c_0 > c_{gel}$ than the determination from settling column tests. Material parameters from settling columns may be used to get a first estimate.

3.3.2 Sensitivity analysis

The sensitivity of the 1DV-slurry model results was evaluated by interchanging the coefficients of the material properties obtained from the different experimental set-ups (SIC and settling). Thus, a computation with c_0 = 200 g/l and the SIC 300 parameters and another one with c_0 = 300 g/l and the SIC 200 parameters were performed. Figure 9 presents these results which show that the model is robust.

3.3.3 Prognostic simulations

The computed evolution of density and effective stress profiles for a 5m high consolidating layer with an initial concentration of

60 g/l are shown in Figure 10. The material parameters are given in Table 3, as determined with the small-scale settling column experiments. Figure 10 shows that the density profile develops from concave- up to concave- down under normal consolidation, and the development of effective stress is also non-linear.

Figure 11 shows the evolution of density profiles from the prognostic simulations starting at concentrations of 175.6 and 558.1 g/l. They correspond with the concentrations after redistribution of the total consolidating sediment mass across the entire thickness of the layer (remixing) at t = 36 h (first phase of consolidation) and t = 1200 days (equilibrium). This redistribution of mass by mixing not only affects the density profile but also the effective stress distribution. The density profile evolution of Figure 11 indicate that further settling occurred after remixing the equilibrium profile of the virgin consolidated suspension. This can be observed in the lowering of the sediment interface. Furthermore, the results show that after remixing at t = 36 h the same final bed height as for the virgin suspension (Figure 10) was obtained (but after a larger consolidation time).
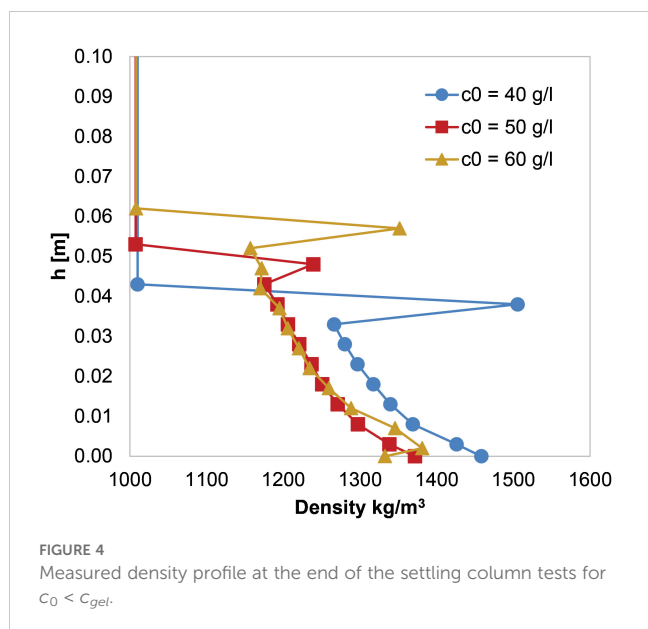
Figure 12 compares the settling curves and final density profiles for all the prognostic simulations. The results show that the final bed height h_∞ for a 5m column suspension with c_0 = 60 g/l was 0.519 m. Remixing the 60 g/l suspension at t=36 h, produced a slurry with c_0 = 175.6 g/l that reached the same final height (h_∞ = 0.506 m).The small difference of these two height values is caused by numerical accuracy (i.e. the interface is detected at one grid cell or at the imminent next one). Finally, remixing the final profile of the virgin consolidated bed formed from the 5m 60 g/l suspension, resulted in a slurry with c_0 = 558.1 g/l and h_∞ =0.469 m. This represents an extra settling of 9.6%. Thus, contrary to remixing at 36 h, remixing at equilibrium did allow further consolidation (multiple grid cells).
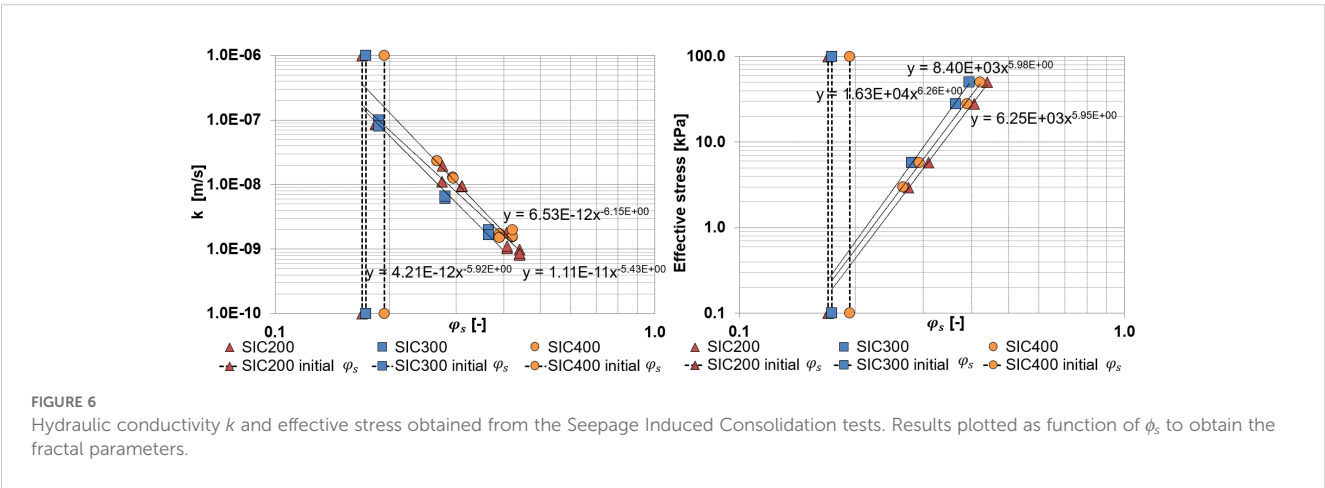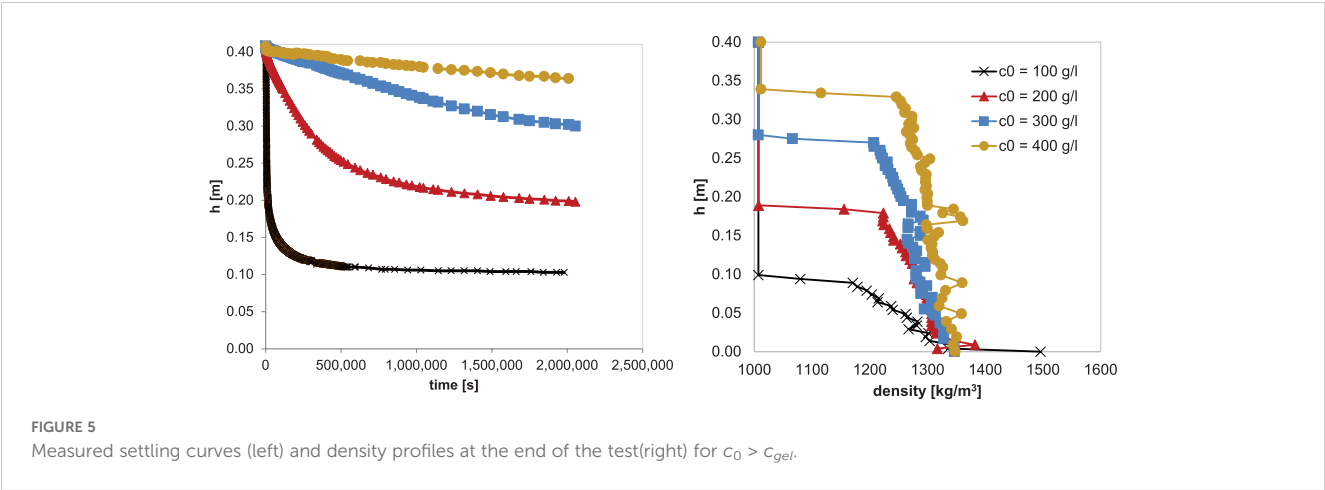
4 Discussion

In this section, the differences between the two experimental set-ups and the effect of mixing and initial concentration on the material parameters are discussed. Furthermore, the change on the stress profile after mixing and the impact of the initial conditions on the final bed density and height are also addressed.

4.1 Non-linearity and the need to use two set-ups

Before discussing the various results in detail it is important to appreciate that the entire consolidation process is extremely non-linear by nature. This can be exemplified from the current results. The stress and strain (permeability) parameters scale with $\phi^{(2/(3-nf))}$, thus $\phi^{6.7}$ for n_f = 2.7, with ϕ the volume concentration of the sediments and nf the fractal dimension. This implies that small inaccuracies in the sediment density and its distribution over the sample have large effects on the accuracy of the experimental stress-strain relations. It is almost impossible to prepare a really homogeneous sample in the triaxial cell of a homogeneous

FIGURE 5
Measured settling curves (left) and density profiles at the end of the test(right) for $c_0 > c_{gel}$.

FIGURE 6
Hydraulic conductivity k and effective stress obtained from the Seepage Induced Consolidation tests. Results plotted as function of ϕ_s to obtain the fractal parameters.

sediment-water suspension in a settling column. The inhomogeneities affect the experimental results in an unknown way. This is one of the reasons why reason a variety of methods two different methods were used to determine the material parameters of the sediment. A second reason is that, settling column tests and SIC tests cover different parts of the effective stress spectrum. In settling columns effective stress remains low (typically less than 1 kPa or even less than 100 Pa, depending on material height) as no loading is applied. In SIC tests the effective stress range larger than 1 kPa is covered. As extrapolation of settling column tests towards a high effective stress range may induce large errors, a combination of SIC tests and settling tests is required to accurately cover the full range of effective stress and

void ratio and to determine k-ϕ and σ_{eff}-ϕ relations that are accurate in a wide range of ϕ.

4.2 Sensitivity of material parameters to initial concentrations

Figure 13 shows the fractal material parameters determined as a function of the initial volumetric concentration of solids $\phi_{s,0}$ for the present research. Herein, the results are also compared to results from Hendriks (2016) and De Lucas Pardo (2015), who both have used similar sediment from lake Markermeer. This figure shows the sensitivity of the K_k parameters to $\phi_{s,0}$, which varies various order of

TABLE 4 Fractal and Liu and Znidarčić (1991) material parameters as obtained from the Seepage Induced Consolidation tests.

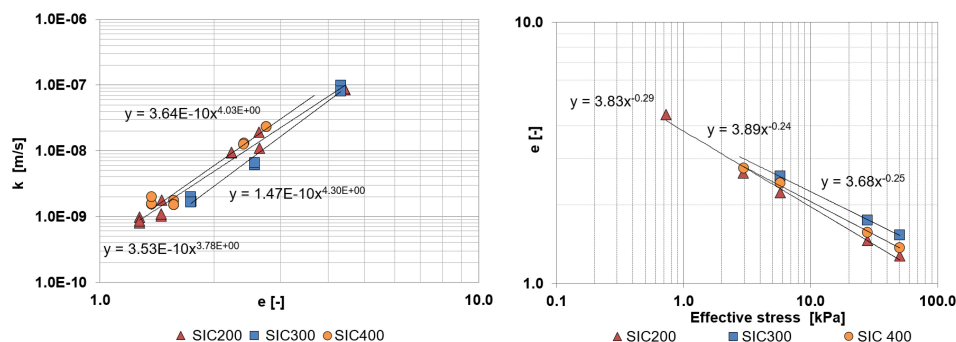| ID	From k data		From σ data		From k data		From σ data	
	n_f [-]	K_k [m/s]	n_f [-]	K_\sigma [Pa]	C_k [m/s]	D_k [-]	A_p [$1/Pa_\sigma^B$]	B_σ [-]
SIC200	2.63	1.11E-11	2.66	6.25E+06	4.00E-10	3.78E+00	3.83	0.29
SIC300	2.66	4.21E-12	2.68	1.63E+07	1.00E-10	4.33E+00	3.89	0.24
SIC400	2.68	6.53E-12	2.67	8.4E+06	4.00E-10	4.04E+00	4.67	0.25

FIGURE 7
Hydraulic conductivity k (left) and effective stress (right) obtained from the Seepage Induced Consolidation tests. Results plotted as function of void ratio to obtain the material parameters according to Liu and Znidarčić (1991). For convenience, the effective stress is presented on the x- axis (see Equation 8).
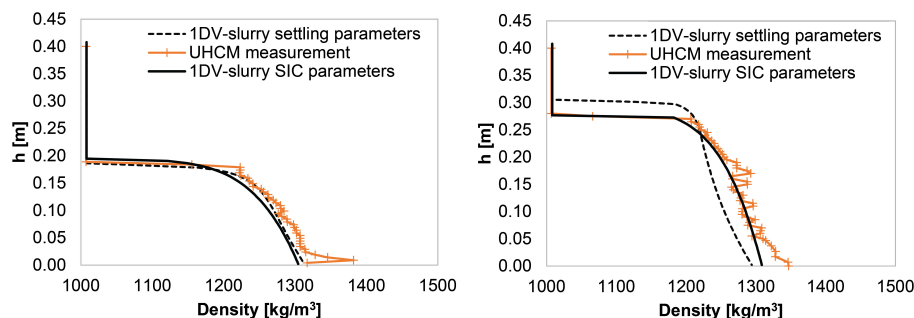

FIGURE 8
Validation of the 1DV-slurry model used for c_0 = 200 g/l (left) and c_0 = 300 g/l (right): measured and computed profiles with SIC and settling column material parameters at t=67 days.

magnitude for different samples. This is different with respect to the K_σ parameter, which values are quite stable. The Liu and Znidarčić (1991) material parameters determined from the SIC test were in the order of magnitude as the ones found previously for Markermeer sediment Van Olphen (2016). They found A_σ=2.55-3.19 [1/Pa$^{B\sigma}$], B_σ= 0.11-0.15 [-], C_k=$1 \cdot 10^{-10}$ $-1 \cdot 10^{-11}$ [m/s] and D_k=6.04-7.00 [-].

The present study demonstrated that the computed profile for an initial concentration of 300 g/L did not achieve the measured equilibrium profile when using parameters obtained from the settling columns ($c_0 < c_{gel}$). However, the equilibrium profile was reached when using the SIC parameters. This discrepancy suggests that the offset may be attributed to the permeability coefficient (K_k) from the settling columns, which was an order of magnitude smaller
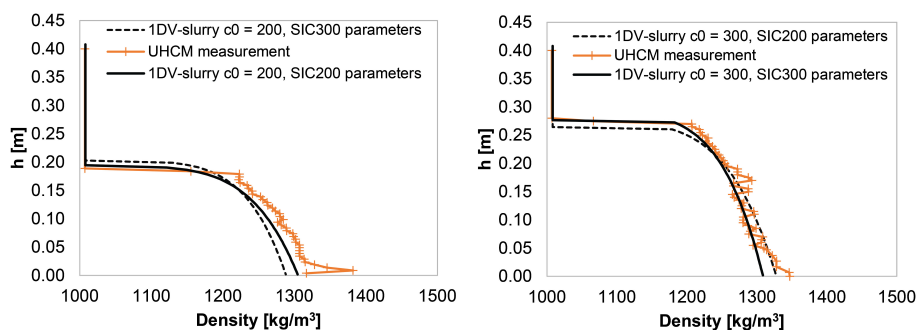

FIGURE 9
Sensitivity analysis. Comparison between the measured density profile and the computed profiles from SIC200 (left) and SIC300 (right), with the parameters of the corresponding tests and after having interchanged parameters.
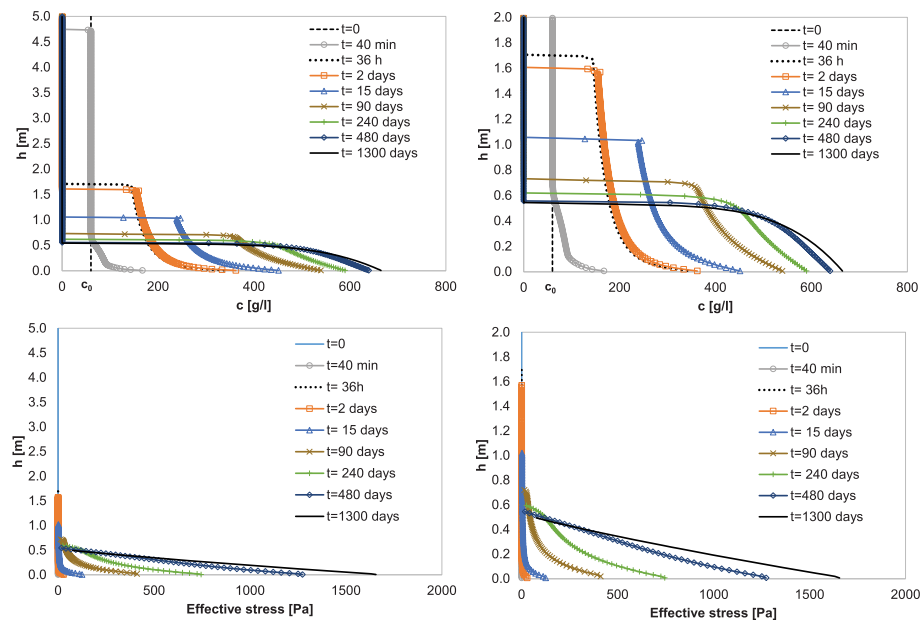
FIGURE 10
Top left panel: Computed density profiles during virgin consolidation of a 5m height column of a suspension with c_0 = 60 g/l. Bottom left panel: effective stress development herein. Right panels are zoom-in.
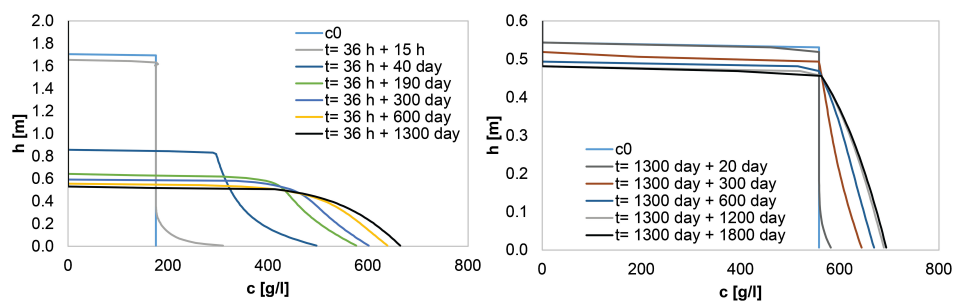

FIGURE 11
Density profiles starting with an initial concentration of 175.6 g/l after remixing the density profile during the first phase of consolidation (at t=36 h of Figure 10) of a suspension (left) and a concentration of 558.1 g/l after remixing the equilibrium profile (t= 1300 days of Figure 10) (right).
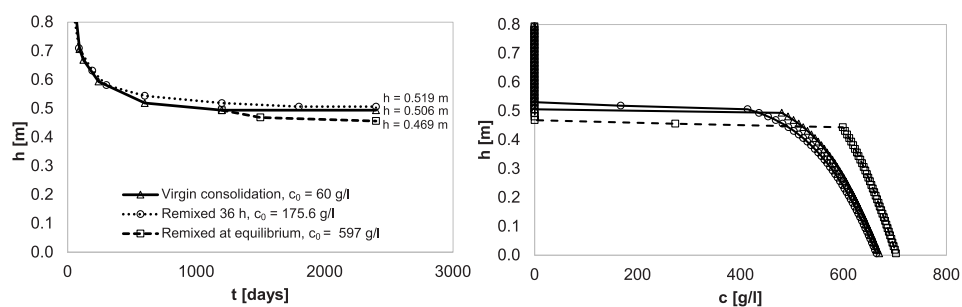
FIGURE 12
Computed settling curves (left) and final concentration profiles (right) for the prognostic simulations.
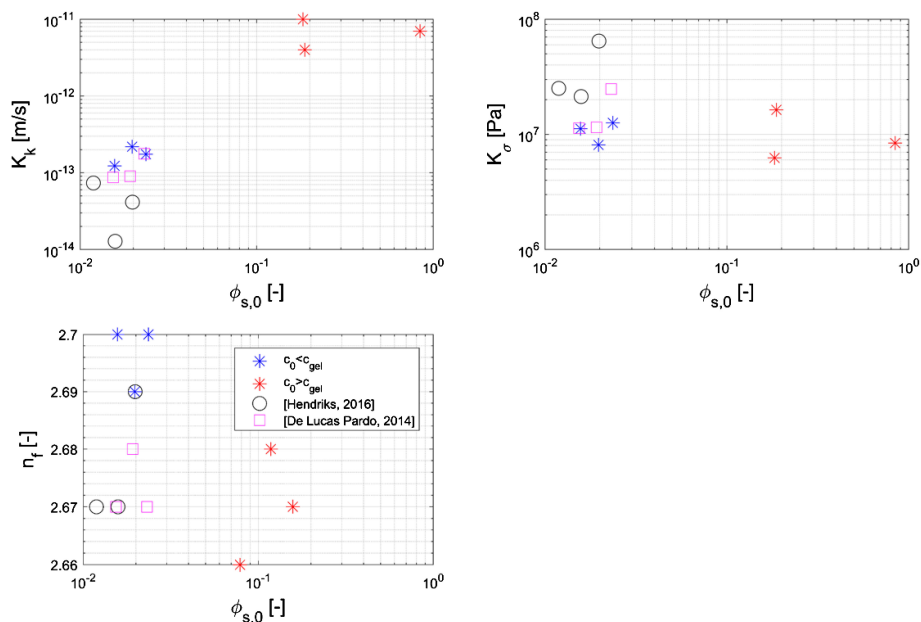
FIGURE 13
Comparison of the fractal material parameters obtained with respect to the initial volumetric concentration, including the results of De Lucas Pardo (2015) and Hendriks (2016).

than the corresponding SIC parameter. Consequently, while final bed heights may be accurately predicted using different sets of material parameters, the consolidation time may vary significantly due to differences in K_k.

4.3 The influence of initial concentration and stress history

In Figure 14, the k and effective stress calculated (Equations 4, 5) with the material parameters obtained from settling tests (Table 3) were extrapolated to ranges of ϕ_s tested with the SIC. This was done to investigate the influence of the $\phi_{s,0}$, mixing and stress history at which the material parameters were determined. The results show that, compared to the extrapolated settling data, the SIC hydraulic

conductivity was larger while the effective stress was smaller (Figure 14). The SIC tests were performed after mixing the sediment of the settling columns. Thus, the results suggest an effect of the mixing and stress history on the parameters determined. In particular, Equations 4, 5 are applied to a more averaged ϕ_s for the case of the SIC. Therefore, the results must differ from the outcome of applying these equations to the settling columns data, where the ϕ_s is not averaged over the vertical. When ϕ_s is almost uniform (SIC tests) through the whole sample, there is almost no gradient of hydraulic conductivity over the vertical. However, if there is a very non uniform ϕ_s distribution through the sample (settling column tests), the gradient of the hydraulic conductivity over the vertical is very large because of the power law that the hydraulic conductivity follows (Equation 4). Given the negative power of this equation, the SIC hydraulic
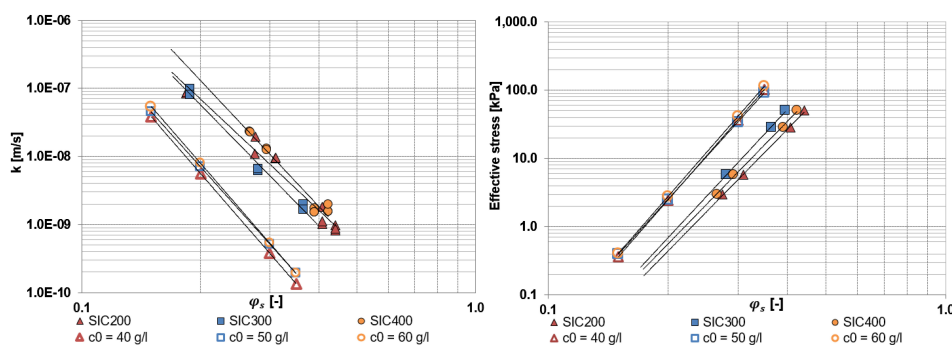

FIGURE 14
Obtained hydraulic conductivity (left) and effective stress (right) from the settling column and SIC tests. The figure includes extrapolated data (to ranges of ϕ_s occurring during the SIC tests) of the k and effective stress obtained from settling column tests.
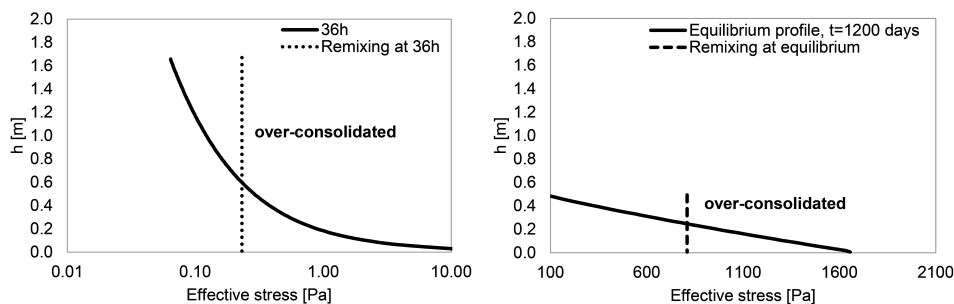
FIGURE 15
Sketch of the change on the stress profile when mixing the sediment with water when dredging. Left panel shows this effect when mixing a virgin consolidating bed at t=36 h (first phase of consolidation). Right panel shows the effect when remixing a virgin bed at equilibrium. Note the different scale of the x-axis.

conductivity obtained from the averaged ϕ_s is larger. In the same way, the positive power of Equation 5 explains the smaller effective stress of the SIC test. Thus, the material parameters behave strongly non-linear. Thus: without mixing (i.e. settling column experiment), the denser material plays relatively a larger role than the less dense material (see Figure 15).

4.4 The effect of the dredging process on the stress profile

The model results indicate that, after mixing, an over- consolidated top layer is present. This is a difference with respect to the hypothetical profile, which represents the stress situation before mixing Markermeer sediment during dredging and pumping. Figure 15 shows the computed effective stress profiles before mixing the consolidating layer at t = 36h and at equilibrium. In this figure, the estimated effective stresses immediately after mixing are also sketched. Herein, the mixing process is expected to disturb the network between particles and to average the concentration through the whole layer. Consequently, the effective stresses at are expected to reduce. Immediately after mixing, the effective stress is constant over the vertical because of the constant volumetric concentration (Equation 5). However, because of the consolidation process and the weight of the uppermost sediment, the effective stresses at the bottom are expected to start increasing rapidly. Finally, Figure 15 also shows that the degree of over- consolidation is different depending on the mixing time.

5 Conclusion

This paper examined the impact of the initial concentration, denoted as c_0, and the stress state post-mixing on the consolidation behaviour of dredged sediment. Dredged sediment is a mixture of sediment and water where $c_0 > c_{gel}$. The study presented two distinct experimental procedures to determine material parameters: settling columns and SIC tests. The material parameters derived from these two setups were not identical, indicating that the stress history, plastic deformation during mixing (when preparing the SIC test sample), or

initial concentration could influence the obtained values. This discrepancy can be attributed to the alteration in the stress state caused by sample homogenisation through mixing. This process results in the existence of an over-consolidated crust-like part relative to the stress profile prior to mixing. This occurs because the mean of the integral of the effective stress does not equate to the integral of the mean of the effective stress. As a result, the values of k obtained from the SIC tests were larger than those determined with the settling columns, while the pattern with the effective stress was the opposite. These differences in material parameters particularly affect the value of K_k and, consequently, the consolidation time. Interestingly, the values of self-similarity (fractal dimension n_f) obtained from both the settling column and SIC tests were identical. A combination of SIC tests and settling tests is essential to accurately encompass the full range of effective stress and void ratio. This approach is necessary to determine the k-ϕ and σ_{eff}-ϕ relationships with precision across a wide range of ϕ.

The initial concentration profile of the sediment plays a significant role in the consolidation behaviour. By dredging and mixing Markermeer sediment, the aforementioned change in the stress state is induced compared to the situation prior to dredging. This process creates over-consolidated initial conditions, which influence the consolidation behaviour and final properties of the sediment. Specifically, the initial concentration affects the final density profile and the final bed height achieved due to varying degrees of over-consolidated initial conditions.

In this context, an initial concentration (c_0) of 558.1 g/l when remixing an equilibrium profile resulted in larger final densities. However, the sediment-water interface was lower, leading to a thinner bed layer. A concentration of 175.6 g/l yielded the same layer thickness and density profile as for virgin consolidation, but required a longer consolidation time.

These factors are particularly crucial for land reclamation and wetland construction, where decisions regarding the initial concentration must be made based on the desired final state. If a thicker final layer is preferred, initial concentrations close to the gelling point (92.2 g/l in this study) are recommended. This condition was achieved with c_0 = 175.6 g/l in this study. However, a very high initial concentration (e.g., c_0 = 558.1 g/l in this research) can yield a denser (and thus stronger) but thinner bed.

Data availability statement

The raw data supporting the conclusions of this article will be made available by the authors, without undue reservation.

Author contributions

Funding

Acknowledgments

Conflict of interest

The authors declare that the research was conducted in the absence of any commercial or financial relationships that could be construed as a potential conflict of interest.

Publisher's note

Supplementary material

The Supplementary Material for this article can be found online at: https://www.frontiersin.org/articles/10.3389/fmars.2024.1466650/full#supplementary-material

References

Abu-Hejleh, A. N., Znidarčić, D., and Barnes, B. L. (1996). Consolidation characteristics of phosphatic clays. *J. Geotech. Eng.* 122, 295–301. doi: 10.1061/(asce)0733-9410(1996)122:4(295

Barciela-Rial, M. (2019). Consolidation and drying of slurries, a Building with Nature study for the Marker Wadden. Delft University of Technology.

Barciela-Rial, M., Saaltink, R., Kessel, T., Chassagne, C., Dekker, S., de Boer, H., et al. (2023). A new setup to study the influence of plant growth on the consolidation of dredged cohesive sediment. *Front. Earth Sci.* 11. doi: 10.3389/feart.2023.952845

Barciela-Rial, M., van Paassen, L., Griffioen, J., Kessel, T., and Winterwerp, J. (2020). The effect of solid-phase composition on the drying behavior of markermeer sediment. *Vadose Zone J.* 19, e20028. doi: 10.1002/vzj2.20028

Barciela-Rial, M., Vardon, P., Kessel, T., Griffioen, J., and Winterwerp, J. (2022). Effect of composition on the compressibility and shear strength of dredged cohesive sediment. *Front. Earth Sci.* 10. doi: 10.1142/12473

Been, K., and Sills, G. C. (1981). Self-weight consolidation of soft soils: an experimental and theoretical study. *Geotechnique´* 31, 519–535. doi: 10.1680/geot.1981.31.4.519

Dankers, P. (2006). On the hindered settling of suspensions of mud and mud-sand mixtures. Delft University of Technology.

Dankers, P., and Winterwerp, J. (2007). Hindered settling of mud flocs: Theory and validation. *Continental Shelf Res.* 27, 1893–1907. doi: 10.1016/j.csr.2007.03.005

De Lucas Pardo, M. (2015). Effect of biota on fine sediment transport processes: A study of Lake Markermeer. Delft University of Technology.

Gibson, R. E., England, G. L., and Hussey, M. J. L. (1967). The theory of one-dimensional consolidation of saturated clays. *Geotechnique´* 17, 261–273. doi: 10.1680/geot.1967.17.3.261

Hendriks, H. (2016). The effect of pH and the solids composition on the settling and self-weight consolidation of mud. Delft University of Technology.

Huerta, A., Kriegsmann, G. A., and Krizek, R. J. (1988). Permeability and compressibility of slurries from seepage-induced consolidation. *J. Geotech. Eng.* 114, 614–627. doi: 10.1061/(ASCE)0733-9410(1988)114:5(614)

Imai, G. (1979). Development of a new consolidation test procedure using seepage force. *Soils Foundations* 19, 45–60. doi: 10.3208/sandf1972.19.345

Kranenburg, C. (1994). The fractal structure of cohesive sediment aggregates. *Estuarine Coast. Shelf Sci.* 39, 451–460. doi: 10.1016/S0272-7714(06)80002-8

Lambe, T. W., and Whitman, R. V. (1969). *Soil Mechanics (Series in Soil Engineering)* (USA: Wiley).

Liu, J. C., and Znidarčić, D. (1991). Modeling one-dimensional compression characteristics of soils. *J. Geotech. Eng.* 117, 162–169. doi: 10.1061/(asce)0733-9410 (1991)117:1(162

Merckelbach, L. M. (2000). Consolidation and strength evolution of soft mud layers. Delft University of Technology.

Merckelbach, L. M., and Kranenburg, C. (2004a). Determining effective stress and permeability equations for soft mud from simple laboratory experiments. *Géotechnique* 54, 581–591. doi: 10.1680/geot.2004.54.9.581

Merckelbach, L. M., and Kranenburg, C. (2004b). Equations for effective stress and permeability of soft mud–sand mixtures. *Géotechnique* 54, 235–243. doi: 10.1680/geot.2004.54.4.235

Sills, B. G. (1998). Development of structure in sedimenting soils. *Philos. Trans. R. Soc. A: Mathematical Phys. Eng. Sci.* 356, 2515–2534. doi: 10.1098/rsta.1998.0284

Terzaghi, K. (1923). Die berechnung der durchlassigkeitzifer des tones aus dem verlauf der hydrodynamischen spannungserscheinungen. mathematish-naturwissenschaftliche, klasse. Part IIa (in German). *Akademie der Wissenschaften Vienna* 132, 125–138.

Terzaghi, K., and Peck, R. (1967). *Soil mechanics in engineering practice. 2nd edition* (New York: John Wiley).

Toorman, E. (1999). Sedimentation and self-weight consolidation: constitutive equations and numerical modelling. *Géotechnique* 49, 709–726. doi: 10.1680/geot.1999.49.6.709

Van Olphen, E. J. C. (2016). Consolidation behaviour of soft cohesive soils, the correlation between different scale model tests: Case study of the Marker Wadden. Delft University of Technology.

Winterwerp, J. (1999). On the dynamic of high-concentrated mud suspensions. Delft University of Technology.

Winterwerp, J., Kessel, T., Maren, D., and Prooijen, B. (2021). *Fine Sediment in Open Water: From Fundamentals to Modeling*. (Singapore: World Scientific). doi: 10.1142/12473

Winterwerp, J. C., and van Kesteren, W. G. (2004). *Introduction to the Physics of Cohesive Sediment Dynamics in the Marine Environment* Vol. 56 (Netherland: Elsevier Science).

Znidarcic, D. (1982). *Laboratory determination of consolidation properties of cohesive soil* (Boulder, Colorado, USA: University of Colorado at Boulder).

Znidarčić, D., and Liu, J. C. (1989). "). Consolidation characteristics determination for dredged materials," in *Proceedings 22nd Annual Dredging Seminar,Ctr. for Dredging Studies* (A&M Univ., College Station, Texas), 45–65.